Nuclear Instruments and Methods in Physics Research A 1092 (2026) 171860

Contents lists available at ScienceDirect

Nuclear Inst. and Methods in Physics Research, A

journal homepage: www.elsevier.com/locate/nima

Full Length Article

Evaluation of dopant removal to design innovative LGADs: Measurements and simulations ☆

A. Fondacci [a,b,*], T. Croci [b], A.R. Altamura [c], R. Arcidiacono [d,c], M. Boscardin [e], N. Cartiglia [c], M. Centis Vignali [e], M. Ferrero [c], S. Galletto [c], L.L. Grimm [f], L. Massaccesi [c], A. Morozzi [b], G. Paternoster [e], D. Passeri [g,b], B. Regnery [f], V. Sola [h,c], R.S. White [c], F. Moscatelli [i,b]

[a] Dipartimento di Fisica, Università degli Studi di Perugia, Via Alessandro Pascoli, 06123, Perugia, Italy
[b] Istituto Nazionale di Fisica Nucleare (INFN) - Sezione di Perugia, Via Alessandro Pascoli, 06123, Perugia, Italy
[c] Istituto Nazionale di Fisica Nucleare (INFN) - Sezione di Torino, Via Pietro Giuria, 1, 10125, Torino, Italy
[d] Dipartimento di Scienze del Farmaco, Università del Piemonte Orientale, Largo Donegani, 2, 28100, Novara, Italy
[e] Fondazione Bruno Kessler (FBK), Via Sommarive, 18, 38123, Trento, Italy
[f] Karlsruhe Institute of Technology, Karlsruhe, Germany
[g] Dipartimento di Ingegneria, Università degli Studi di Perugia, Via Goffredo Duranti, 93, 06125, Perugia, Italy
[h] Dipartimento di Fisica, Università degli Studi di Torino, Via Pietro Giuria, 1, 10125, Torino, Italy
[i] Istituto Officina dei Materiali (IOM) CNR - Sede di Perugia, Via Alessandro Pascoli, 06123, Perugia, Italy

ARTICLE INFO

Keywords:
Low-gain Avalanche diodes
Dopant removal
Van der Pauw
Sheet resistance
TCAD simulations

ABSTRACT

The development of innovative Low-Gain Avalanche Diode architectures has required the characterisation of dopant removal at high initial concentrations. In this contribution, dopant removal is investigated using sheet resistance measurements on dedicated van der Pauw test structures. Donor removal coefficients are extracted for NPLUS implants at initial concentrations exceeding 10^{18} cm^{-3}. The acceptor removal coefficient is also directly extracted for the PPLUS implant and validated by means of TCAD simulations, in which a SIMS-based process simulation scaled according to the extracted coefficient reproduces the measured evolution of the sheet resistance with irradiation. The results show that donor removal proceeds approximately a factor of 2–3 faster than acceptor removal, also at high initial dopant concentrations.

1. Introduction

The development of innovative Low-Gain Avalanche Diode (LGAD) architectures, such as resistive LGADs [1] and compensated LGADs [2], has highlighted the importance of understanding and characterising donor removal at concentrations much higher than those traditionally used in n-type substrates [3], since donor implants are central to their operation. Resistive LGADs achieve micrometre-scale position resolution with pixel pitches of several hundred micrometres via intrinsic signal sharing, enabled by the n-doped resistive collection electrode. Meanwhile, in compensated LGADs, which are regarded as promising candidates for 4D tracking at extreme fluences ($\geq 10^{17}$ 1 MeV n_{eq} cm^{-2}), the gain layer is realised through a carefully engineered compensation of acceptor and donor dopants.

In this framework, a new technique [4] has recently been explored to characterise dopant removal, both acceptor and donor. This method measures irradiation-induced changes in sheet resistance using dedicated van der Pauw (vdP) test structures [5], and has already been experimentally applied to resistive LGAD samples from the Fondazione Bruno Kessler (FBK) RSD2 batch [6]. The donor removal coefficients derived from these measurements have been validated through Technology Computer-Aided Design (TCAD) simulations [7], demonstrating the effectiveness of the technique in studying dopant removal in implants with a peak concentration close to the surface and of opposite type with respect to the substrate.

This contribution presents an experimental application of the method to extract additional donor removal coefficients from the NPLUS implant using resistive LGAD samples from the FBK DCRSD1 batch [8], thereby extending the available data on donor removal at high initial donor concentrations ($\geq 10^{18}$ cm^{-3}). In addition, the method is applied to implants with peak concentrations near the

☆ This article is part of a Special issue entitled: '2025 HSTD14' published in Nuclear Inst. and Methods in Physics Research, A.

* Corresponding author at: Istituto Nazionale di Fisica Nucleare (INFN) - Sezione di Perugia, Via Alessandro Pascoli, 06123, Perugia, Italy.
E-mail address: alessandro.fondacci@pg.infn.it (A. Fondacci).

https://doi.org/10.1016/j.nima.2026.171860
Received 24 March 2026; Received in revised form 26 June 2026; Accepted 5 July 2026
Available online 10 July 2026

surface and of the same type as the substrate. Specifically, the high-concentration acceptor-type PPLUS implant is analysed, allowing the comparison between donor and acceptor removal previously reported in [4] to be revisited in a high initial doping concentration regime. The investigation of acceptor removal at high initial concentrations is of particular relevance for compensated LGAD architectures, where the gain layer is realised through a finely engineered compensation between high-dose acceptor and donor implants, making the radiation-induced deactivation of both dopant species a critical design parameter.

2. Donor removal in high-concentration NPLUS implants

In FBK terminology, the NPLUS implant denotes the donor-doped layer used to form the collection electrode. In resistive LGADs, this implant is intentionally less doped than in standard LGADs in order to provide a higher sheet resistance. In the DCRSD1 batch, the same three relative NPLUS implantation doses employed in the RSD2 batch were used. Since the absolute implantation doses are proprietary FBK process information, they are reported as dimensionless dose factors normalised to the highest dose: 0.25, 0.50, and 1.00, corresponding respectively to one quarter, one half, and the reference dose. The DCRSD1 batch, however, features silicon oxide trenches, which impose a reduced thermal budget during fabrication and consequently result in a higher donor concentration for a given relative NPLUS implantation dose with respect to the RSD2 batch. For this reason, NPLUS vdP test structures from the DCRSD1 batch were irradiated and electrically characterised in order to extract donor removal coefficients corresponding to higher initial donor concentrations than those previously obtained from RSD2 samples. Neutron irradiation was performed at the JSI TRIGA reactor at fluences of 0.5, 1.0, and 1.5×10^{15} 1 MeV n_{eq} cm^{-2}.

Fig. 1 shows the measured sheet conductance, defined as the inverse of the sheet resistance, as a function of fluence for the different NPLUS implantation doses, indicated by markers of different colours. All measurements were performed at room temperature in the INFN Perugia cleanroom, both before and after irradiation. Following the procedure described in Appendix A of [4], a known current ramp was applied between two adjacent electrodes of a four-terminal vdP test structure, while the voltage drop across the remaining two electrodes was recorded. The sheet resistance was obtained from the slope of the voltage–current characteristic, multiplied by the factor $\pi / \ln(2)$, and the corresponding sheet conductance was calculated as its inverse. The current ramp was set to ± 1 mA in order to keep the measured voltage drop within the 1–100 mV range. The probe-station chuck was left floating, since back-side biasing is not envisaged in vdP measurements. Each marker represents the average of at least five measurements performed on vdP test structures from W3, W14, and W15 for the relative NPLUS doses of 0.25, 0.50, and 1.00, respectively. The corresponding DCRSD1 batch split table is reported in [8].

The donor removal coefficient, c_D, which quantifies the deactivation rate of electrically active donor atoms into complex neutral defects induced by irradiation, can be extracted from the sheet conductance measurements by means of an exponential fit, as shown in Fig. 1.

The fluence dependence of the electrically active donor concentration can be parameterised through an exponential removal law [9],

$$N_D(\phi) = N_D(0)\, e^{-c_D\, \phi}, \tag{1}$$

where ϕ denotes the irradiation fluence expressed in 1 MeV n_{eq} cm^{-2}, and $N_D(\phi)$ and $N_D(0)$ are the active donor concentrations after irradiation at fluence ϕ and before irradiation, respectively.

Given that the sheet conductance is directly proportional to the concentration of electrically active donors—corresponding to the majority carriers in the case of the NPLUS implant—the same exponential dependence is expected for the measured sheet conductance as a function of fluence. Consequently, the donor removal coefficient c_D can be directly extracted by performing an exponential fit to the experimental sheet conductance data.

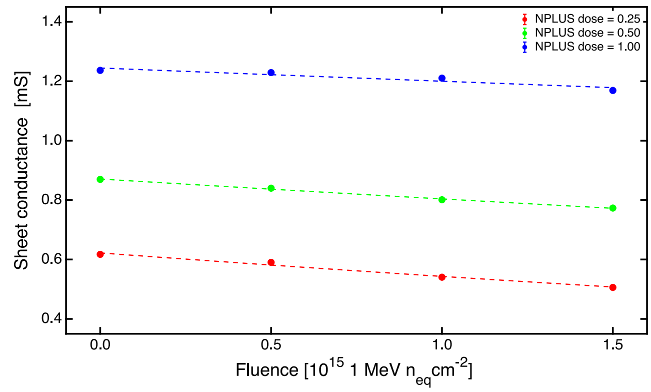

Fig. 1. Experimental sheet conductance measured on vdP test structures for three relative NPLUS implantation doses (colour-coded markers) before irradiation and after neutron irradiation at the JSI TRIGA reactor at fluences of 0.5, 1.0, and 1.5×10^{15} 1 MeV n_{eq} cm^{-2}. Error bars represent the standard error of the mean and are generally smaller than the marker size. Dashed lines indicate exponential fits used to determine the donor removal coefficients.

By applying this procedure to the measurements, the extracted donor removal coefficients are $(1.4 \pm 0.3) \times 10^{-16}$ cm^2, $(0.8 \pm 0.1) \times 10^{-16}$ cm^2, and $(0.4 \pm 0.2) \times 10^{-16}$ cm^2 for relative NPLUS implantation-dose factors of 0.25, 0.50, and 1.00, respectively. These values are reported in Fig. 5 as blue square markers and show good agreement with the donor removal coefficients previously extracted from RSD2 samples (magenta square markers), despite the different fabrication thermal budgets and resulting initial donor concentrations.

3. Acceptor removal in high-concentration PPLUS implant

The donor removal coefficients extracted for the NPLUS implant extend the experimental knowledge of donor removal into a high initial doping concentration regime ($\geq 10^{18}$ cm^{-3}), made accessible by the van der Pauw (vdP) method. In this concentration range, while donor removal can now be directly determined from experimental data, the corresponding acceptor removal behaviour is still only described through extrapolations based on capacitance–voltage measurements performed at lower initial concentrations, of the order of 10^{16} cm^{-3}, relevant for LGAD gain-layer implants.

In order to enable a meaningful comparison between donor and acceptor removal at high dopant concentrations, and to assess the predictive power of such extrapolations, the vdP method is here applied to the PPLUS implant. The PPLUS implant is characterised by a very high initial acceptor concentration and is employed to allow sensor biasing from the top side rather than through the substrate.

PPLUS vdP test structures from the 30 μm-thick EXFLU1 wafers were neutron irradiated at the JSI TRIGA reactor at fluences of 0.4, 0.8, 1.2, 1.5, 2.5, and 3.5×10^{15} 1 MeV n_{eq} cm^{-2}, and subsequently electrically characterised at room temperature. Reliable pre-irradiation sheet-resistance measurements could not be obtained for these structures; therefore, no point at zero fluence is reported in Fig. 2. Fig. 2 reports the measured sheet conductance as a function of fluence. Each marker represents the average over multiple test structures irradiated at the same fluence and originating from different wafers, since no dedicated process split was implemented for the PPLUS implant. The measurement procedure is identical to that described for the NPLUS samples.

The irradiation-induced deactivation of electrically active acceptors—corresponding to the majority carriers in the case of the PPLUS implant—can be parameterised using the same exponential removal law introduced for donors in Eq. (1). Under the assumption that the sheet conductance is directly proportional to the concentration

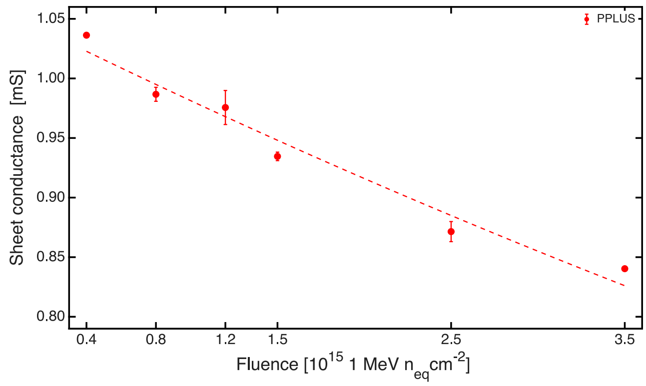

Fig. 2. Experimental sheet conductance measured on van der Pauw test structures of the PPLUS implant as a function of neutron irradiation fluence. The samples were irradiated at the JSI TRIGA reactor at fluences of 0.4, 0.8, 1.2, 1.5, 2.5, and 3.5×10^{15} 1 MeV n_{eq} cm^{-2}. Error bars represent the standard error of the mean and, where not visible, are smaller than the marker size. A dashed line indicates the exponential fit used to determine the acceptor removal coefficient.

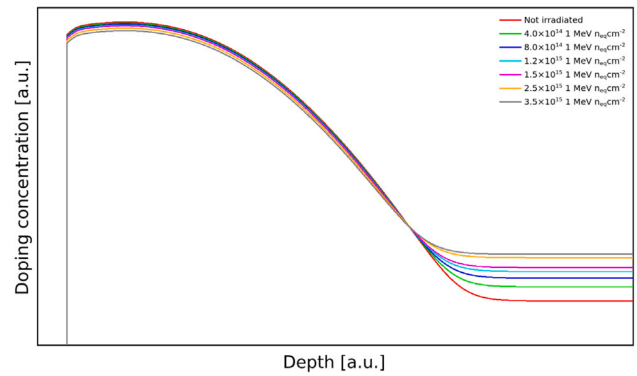

Fig. 3. TCAD-simulated evolution of the doping profile with irradiation. The PPLUS acceptor concentration is reduced according to Eq. (2), using the experimentally extracted acceptor removal coefficient $c_A = 0.8 \times 10^{-16}$ cm^2. The increase of the substrate acceptor concentration due to irradiation is modelled following the acceptor creation parametrisation reported in [10].

of electrically active acceptors, the acceptor removal coefficient c_A can therefore be extracted by performing an exponential fit to the measured sheet conductance as a function of fluence.

The extracted acceptor removal coefficient is $c_A = (0.8 \pm 0.2) \times 10^{-16}$ cm^2. As previously done for the donor removal coefficients, a TCAD-based validation is required in order to confirm the capability of the vdP method to correctly extract dopant removal coefficients also in the case of implants having the same conductivity type as the substrate.

For this purpose, a Secondary Ion Mass Spectrometry (SIMS)-based process simulation of the PPLUS implant was implemented and scaled according to the extracted acceptor removal coefficient following the exponential law

$$N_A(\phi) = N_A(0)\, e^{-c_A \phi}, \tag{2}$$

where ϕ denotes the irradiation fluence expressed in 1 MeV n_{eq} cm^{-2}, and $N_A(\phi)$ and $N_A(0)$ are the active acceptor concentrations after irradiation at fluence ϕ and before irradiation, respectively. The pre-irradiation process simulation was calibrated using measurements from 45 µm-thick EXFLU1 wafers, for which reliable unirradiated data were available.

Fig. 3 shows the evolution with irradiation of the PPLUS doping profile used in the TCAD simulations. In addition to the reduction of the PPLUS implant, acceptor creation in the substrate [10] was included. Radiation damage in both the bulk and at the surface was modelled using the New University of Perugia defect model [11].

In contrast to the TCAD validation performed for the NPLUS RSD2 samples, where an analytical approach was used to compute the sheet resistance, the case of the PPLUS implant requires a different strategy. The sheet resistance can be expressed analytically as

$$R_{sh} = \frac{1}{\int_0^d q\left[n(x)\mu_n(x) + p(x)\mu_p(x)\right]\,dx}, \tag{3}$$

where q is the elementary charge, n and p are the electron and hole concentrations, μ_n and μ_p are the corresponding mobilities, and d is the junction depth. While carrier concentrations and mobilities are directly accessible in the TCAD environment, the definition of the junction depth becomes ambiguous for a p-type implant realised on a p-type substrate.

For this reason, a full three-dimensional vdP test structure was explicitly reproduced in the TCAD simulation domain, and the experimental measurement procedure was replicated in simulation in order to extract the sheet resistance. This approach also allows the parasitic contribution of the substrate to be naturally taken into account, since the implant under test is no longer electrically isolated from the substrate by a space-charge region.

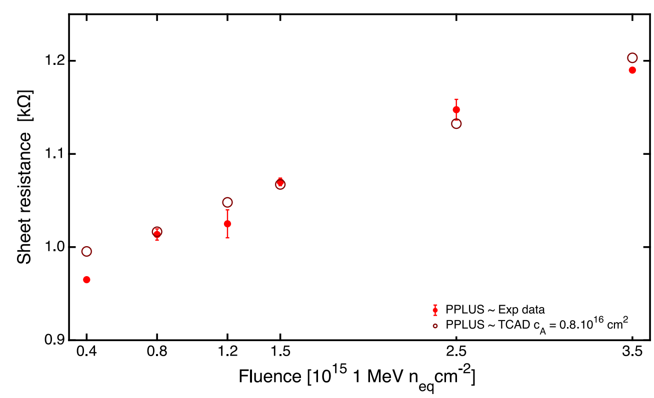

Fig. 4. Comparison between measured and TCAD-simulated sheet resistance as a function of neutron fluence for the EXFLU1 PPLUS implant. Experimental data are shown as filled markers, while TCAD simulation results are represented by open markers. Error bars on the experimental data represent the standard error of the mean.

Fig. 4 compares the simulated and measured PPLUS sheet resistance as a function of fluence. The good agreement between simulation and measurements validates the vdP method for extracting dopant removal coefficients also in the case of high-concentration implants with peak doping close to the surface and of the same conductivity type as the substrate.

The experimentally extracted and TCAD-validated acceptor removal coefficient c_A can now be directly compared with the donor removal coefficients c_D obtained from the NPLUS samples. This comparison is shown in Fig. 5, where the extracted c_A is represented by an open blue diamond marker. The figure also reports the comparison previously obtained at lower initial doping concentrations, showing that donor removal is consistently a factor of 2–3 faster than acceptor removal.

This result confirms the correlation between dopant removal coefficients extracted from sheet resistance measurements at high doping concentrations and those obtained from capacitance measurements at lower concentrations. Such correlation was already demonstrated in [4], where a SIMS-based process simulation of the PGAIN implant, scaled according to the acceptor removal parametrisation derived from capacitance measurements, successfully reproduced the measured evolution of the sheet resistance with irradiation.

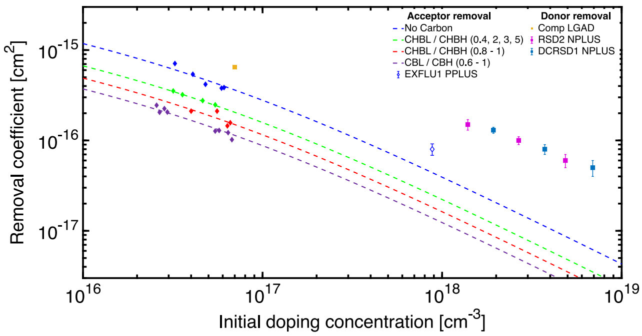

Fig. 5. Acceptor and donor removal coefficients as a function of the initial doping concentration. Filled diamond markers represent acceptor removal coefficients extracted from capacitance measurements on LGADs with different gain implants. Dashed lines represent the corresponding parametrisations reported in [10]; each line refers to the group of filled diamond markers of the same colour. The open blue diamond marker corresponds to the acceptor removal coefficient extracted from sheet resistance measurements of the PPLUS implant. Square markers indicate donor removal coefficients: the yellow square is obtained from the comparison between capacitance measurements and simulations of compensated LGADs, while magenta and blue squares are extracted from sheet resistance measurements of NPLUS implants. Error bars represent the 95% confidence intervals of the removal coefficients extracted from the fits.

4. Conclusion

In this contribution, dopant removal at high initial concentrations relevant for innovative LGAD architectures has been investigated using sheet resistance measurements on dedicated van der Pauw test structures. The method has been applied to both donor- and acceptor-type implants with peak concentrations close to the surface, enabling the experimental study of dopant removal in regimes not accessible through standard capacitance-based techniques.

Donor removal coefficients have been experimentally extracted for DCRSD1 NPLUS implants at initial concentrations exceeding 10^{18} cm^{-3} by applying the van der Pauw method. The validity of this approach for donor-type surface implants on p-type substrates had been previously demonstrated through TCAD simulations on RSD2 NPLUS van der Pauw test structures. In contrast, for the PPLUS implant the acceptor removal coefficient has been directly extracted from sheet resistance measurements and subsequently validated in this contribution by means of TCAD simulations. In this case, a SIMS-based process simulation of the PPLUS implant, scaled according to the experimentally extracted acceptor removal coefficient, was shown to accurately reproduce the measured evolution of the sheet resistance with irradiation. The comparison between donor and acceptor removal confirms that donor deactivation proceeds approximately a factor of 2–3 faster than acceptor deactivation, consistently with trends previously inferred at lower doping concentrations.

Further extensions of this study will be enabled by the new NLGAD batch, manufactured by FBK, which will allow additional donor removal coefficients to be extracted at initial concentrations around 10^{16} cm^{-3}. In this case, the applicability of the van der Pauw method will be investigated for implants characterised by a doping peak located deeper in the bulk rather than at the Si–SiO_2 interface, and by a reduced ratio between the peak concentration and the substrate doping.

Declaration of competing interest

The authors declare that they have no known competing financial interests or personal relationships that could have appeared to influence the work reported in this paper.

Acknowledgements

This project has received funding from the European Union's Horizon 2020 Research and Innovation Programme under GAs Nos 101004761 (AIDAinnova) and 101057511 (EURO-LABS), the European Union – Next Generation EU, Mission 4 Component 1 CUP D53D23002870001 (Comon-Sens), and the European Union (ERC, CompleX, 101124288). Views and opinions expressed are however those of the authors only and do not necessarily reflect those of the European Union or the European Research Council. Neither the European Union nor the granting authority can be held responsible for them.

This work has also received funding from INFN CSN5 through the 4DSHARE research project; from PRIN MIUR projects 2017L2XKTJ ("4DInSiDe") and 2022KLK4LB ("4DSHARE").

References

[1] M. Tornago, et al., Resistive AC-Coupled Silicon Detectors: Principles of operation and first results from a combined analysis of beam test and laser data, Nucl. Instrum. Meth. A 1003 (2021) 165319, http://dx.doi.org/10.1016/j.nima.2021.165319.

[2] V. Sola, et al., A compensated design of the LGAD gain layer, Nucl. Instrum. Meth. A 1040 (2022) 167232, http://dx.doi.org/10.1016/j.nima.2022.167232.

[3] R. Wunstorf, et al., Investigations of donor and acceptor removal and long term annealing in silicon with different boron/phosphorus ratios, Nucl. Instrum. Meth. A 377 (1996) 228–233, http://dx.doi.org/10.1016/0168-9002(96)00217-3.

[4] A. Fondacci, et al., Compensated LGAD optimisation through van der Pauw test structures, Nucl. Instrum. Meth. A 1080 (2025) 170800, http://dx.doi.org/10.1016/j.nima.2025.170800.

[5] L.J. van der Pauw, A method of measuring specific resistivity and hall effect of discs of arbitrary shape, in: Semiconductor Devices: Pioneering Papers, pp. 174–182, http://dx.doi.org/10.1142/9789814503464_0017.

[6] U. Elicabuk, et al., Irradiation studies of the Resistive AC-Coupled Silicon Detector (RSD/AC-LGAD), Nucl. Instrum. Meth. A 1080 (2025) 170705, http://dx.doi.org/10.1016/j.nima.2025.170705.

[7] A. Fondacci, et al., Next-generation LGADs: a measurement-simulation synergy to quantify donor removal, PoS VERTEX2025 (2025) 023, http://dx.doi.org/10.22323/1.513.0023.

[8] R. Arcidiacono, et al., Innovative DC-coupled resistive silicon detector for 4D tracking, Nucl. Instrum. Meth. A 1080 (2025) 170796, http://dx.doi.org/10.1016/j.nima.2025.170796.

[9] M. Moll, et al., Investigation on the improved radiation hardness of silicon detectors with high oxygen concentration, Nucl. Instrum. Meth. A 439 (2000) 282–292, http://dx.doi.org/10.1016/S0168-9002(99)00842-6.

[10] M. Ferrero, et al., Radiation resistant LGAD design, Nucl. Instrum. Meth. A 919 (2019) 16–26, http://dx.doi.org/10.1016/j.nima.2018.11.121.

[11] A. Morozzi, et al., TCAD simulations for radiation-tolerant silicon sensors, PoS VERTEX2023 (2024) 060, http://dx.doi.org/10.22323/1.448.0060.